Polytypism of Crystals of Tin Disulphide; Structures of 21 Polytypes of SnS₂

By B. Pałosz, W. Pałosz* and S. Gierlotka

Institute of Physics, Warsaw Technical University, 00 662 Warszawa, ul.Koszykowa 75, Poland

Abstract. The polytype structure of SnS₂ crystals grown by chemical transport is discussed: large polytype cells of SnS₂ are presented as multiphase (interpolytype) structures intermediate between basic polytypes 2H, 4H and 18R. Polytypism of SnS₂ is compared with polytypism of CdI₂ and other MX_2 crystals. Structures of 21 large-period polytypes of SnS₂ are presented: hexagonal polytypes: $10H_1$: $tf5tf1f1$; $14H_1$: $tf5tf1(o)_2f1$; $20H_1$: $(f1f5f1)_3o$; $26H_1$: $(t)_2(f5f1of1)_2f5f1f1$; $30H_1$: $(f1f5f1o)_2f1f5f1(o)_4$; $38H_1$: $(f1f5f1)_6o$; $40H_1$: $(f1f5f1)_6(o)_2$; $56H_1$: $(f1f5f1)_9o$; $74H_1$: $(f1f5f1)_{12}o$; rhombohedral polytypes: $24R_1$: $f1f5f1o$; $30R_1$: $f1f5f1(o)_2$; $42R_1$: $f1f5f1(o)_4$; $48R_1$: $f1f5f1(o)_5$; $66R_1$: $f1f5f1of1f5f1(o)_4$; $66R_2$: $(t)_2f5f1(o)_2f1f5f1of1$; $78R_1$: $f1f5f1(o)_{10}$; $78R_2$: $f1f5f1(o)_3f1f5f1(o)_4$; $84R_1$: $(f1f5f1)_4(o)_2$; $102R_1$: $f1f5f1(o)_{14}$; $132R_1$: $f1f5f1(o)_5f1f5f1(o)_{11}$; $156R_1$: $(f1f5f1)_6o(f1f5f1)_2o$.

Introduction. Tin disulphide belongs to a family of crystals of the type MX_2 exhibiting structural polytypism: CdI₂, PbI₂, CdBr₂, SnSe₂, Ti₁.₂S₂. Of these the structure of CdI₂ is relatively best explored: the structures of more than 200 polytypes of CdI₂ have been determined. Amongst others, 16 and 11 structures of PbI₂ and Ti₁.₂S₂, respectively, have been determined. Although multilayer polytypes of SnS₂ were reported by Mitchell, Fujiki & Ishizawa (1974), Whitehouse & Balchin (1979a) and Minagawa (1980) the layer sequences for these polytypes were not identified.

Crystals of SnS₂ can adopt three different basic structures: 2H, 4H and 18R. The structures of these polytypes have been determined uniquely by single-crystal X-ray diffraction by Whitehouse & Balchin (1979a). Their Zhdanov sequences are: 2H 11, 4H 22, 18R (1212)₃. It was found that crystals grown from the melt by the Bridgman method have only the structure 4H while those grown by chemical transport tend to exhibit polytypism (Minagawa, 1980). In this case the polytypes 2H, 4H and 18R form simultaneously and their relative frequencies of occurrence change depending on growth conditions. The effect of growth

parameters on the formation of basic structures and of multilayer polytypes has not been established as yet. Polytypism was observed in crystals obtained during iodine transport from 973 to 873 K (Mitchell *et al.*, 1974), from 953 to 913 K (Minagawa, 1980) and from 960 to 920 K (Whitehouse & Balchin, 1979a). Recently we began a systematic study of the structure of SnS₂ crystals grown at different temperatures from about 673 to about 1173 K and we found a number of multilayer polytypes with cells having from eight to a few hundred layers. Below we present the results of X-ray investigations of polytypes of SnS₂ and the structures of 21 polytypes for which we determined the sequences of layers in the cells.

Experimental. Crystals of SnS₂ were grown from the vapour phase by the method of chemical transport. Starting materials were SnS₂ and SnI₄ powders prepared by a method similar to that described by Wiedemeier & Csillag (1979). Growth experiments were performed in closed silica ampoules of inner diameter 10–15 mm and of length 8–13 cm. The ampoules were charged with 2–3 g of SnS₂ and with the desired amount of SnI₄ powder. An average concentration of transporting agent was 8 mg cm⁻³. The ampoules were evacuated to about $1 \cdot 3 \times 10^{-2}$ Pa and sealed off. After about 1 d of reverse transport the ampoules were placed in the desired position in a furnace. The temperature of the charge was in the range 850–1020 K; undercooling was 10–30 K. After 1–4 d the ampoules were pulled out of the furnace and allowed to cool to room temperature. Golden-yellow plate-shaped single crystals with dimensions from $1 \times 1 \times 0 \cdot 01$ mm to $10 \times 20 \times 0 \cdot 5$ mm were obtained. Growth temperatures for the polytypes of SnS₂ under investigation are given in Table 1.

To identify polytypes measurements of the relative intensities and positions of a relatively small number of characteristic reflexions (*e.g.* 10.*l*, 20.*l*, 1 $\bar{1}$.*l etc.*) are sufficient to determine the space group and the stackings of layers in a polytype cell (Verma & Krishna, 1966). To register these reflexions either *c*-, *a*- or *a**-axis Weissenberg or oscillation photographs may be used. For the identification of SnS₂ polytypes we adopt the method of structural analysis used successfully for the determination of more than 120

---

* Present address: Department of Chemistry, Rensselaer Polytechnic Institute, Troy, NY 12181, USA.

Table 1. *Structure and growth conditions of* 21 *polytypes of tin disulphide*

Ramsdell symbol	*t–o–f* sequence of a cell	Temperature of growth (K)	Series (Table 2)
Hexagonal polytypes			
$10H_1$	$tf5tf1f1$	1203	SnH–4
$14H_1$	$tf5tf1(o)_2f1$	1203	SnH–4
$20H_1$	$(f1f5f1)_2f1f5f1o$	843, 873	SnH–1
$26H_1$	$(t)_2f5f1(of1f5f1)_2f1$	843	SnH–3
$30H_1$	$(f1f5f1o)_2f1f5f1(o)_4$	873	SnH–1
$38H_1$	$(f1f5f1)_3f1f5f1o$	873	SnH–1
$40H_1$	$(f1f5f1)_3f1f5f1(o)_2$	873	SnH–1
$56H_1$	$(f1f5f1)_8f1f5f1o$	918	SnH–1
$74H_1$	$(f1f5f1)_{11}f1f5f1o$	918	SnH–1
Rhombohedral polytypes			
$24R_1$	$f1f5f1o$	873, 918	SnR–1
$30R_1$	$f1f5f1(o)_2$	843, 873	SnR–1
$42R_1$	$f1f5f1(o)_4$	873	SnR–1
$48R_1$	$f1f5f1(o)_5$	873	SnR–1
$66R_1$	$f1f5f1(o)_4f1f5f1o$	843	SnR–2
$66R_2$	$f1(o)_2f5f1(o)_2f1f5f1o$	873	SnR–2
$78R_1$	$f1f5f1(o)_{10}$	873	SnR–1
$78R_2$	$f1f5f1(o)_3f1f5f1(o)_4$	873	SnR–2
$84R_1$	$(f1f5f1)_3f1f5f1(o)_2$	918	SnR–1 + SnR–2
$102R_1$	$f1f5f1(o)_{14}$	873	SnR–1
$132R_1$	$f1f5f1(o)_3f1f5f1(o)_{11}$	793	SnR–2
$156R_1$	$(f1f5f1)_3f1f5f1of1f5f1f1f5f1o$	918	SnR–1 + SnR–2

polytypes of CdI_2: Pałosz (1982a, 1983a), Pałosz & Gierlotka (1984). In this method we divided the polytypes into four groups corresponding to four kinds of symmetry of diffraction patterns, identifying, in this way, some specific arrangements of layers occurring in the crystals. To use this classification the reflexions $10.l$ and $10.\bar{l}$ (or $1\bar{1}.l$) for which l varies between $n \times N + N/2$ and $n \times N - N/2$ ($n = 0, 1, 2, \ldots$; N is the number of layers X in a cell) should be measured experimentally (Pałosz & Przedmojski, 1980; Pałosz, 1980). We found that for SnS_2 these reflexions are observed on 15° a^*-axis oscillation patterns when $Co\,K$ radiation was used and when the angle between the c axis and the incident beam varies between 15 and 30°. A cylindrical camera with radius 43 mm and a 0·7 mm collimator was used.

The intensity values for the reflexions $10.l$ and $1\bar{1}.l$ for the theoretical models of SnS_2 polytypes have been computed using the standard expression for MX_2 crystals, e.g. Gyaneshwar, Chadha & Trigunayat (1973). The f_S and f_{Sn} factors were approximated by the analytical function given by Lee & Pakes (1969). The reflexion intensities so calculated were multiplied by the Lorentz–polarization factor Lp^{-1}. As discussed by Whitehouse & Balchin (1979b) a unique identification of MX_2 polytypes needs the use of an absorption correction factor A. The use of absorption corrections is, in the case of the back-reflexion technique, very troublesome because, to derive correct values of this factor, accurate information regarding the position of reflexion, and the shape and dimensions of the sample are required. As the shape and dimensions change from crystal to crystal, the relative intensities of the reflexions registered for the same polytype but occurring in different crystals are, in general, different. Because of this, here the absorption corrections were used to normalize the experimental intensity patterns; the reflexion intensities (measured by photometry) were multiplied by the factor A^{-1} appropriate to the shape of the specimen.

Construction of polytypes of SnS_2. Series of polytypes

The structure of a polytype may be represented by several methods of symbolic notation of their layered structure. For MX_2 crystals notations based on the sequence of monoatomic layers $ABC\alpha\beta\gamma$ (Hägg, Zhdanov, *hc* notations: Verma & Krishna, 1966) and based on molecular-layer X–M–X stackings ($\alpha\beta\gamma$ and thr: Fichtner 1982, 1983; xyz and t–o–f notations: Pałosz, 1980) were suggested. Of these methods the t–o–f notation appeared most useful for the identification of CdI_2 polytypes (Pałosz, 1982a, 1983a; Pałosz & Gierlotka, 1984) and this notation is used here for the SnS_2 polytypes.

As was shown for CdI_2 and PbI_2 by Pałosz (1983c), multilayer polytypes occurring in real crystals and having complex cells may always be considered as structures composed of basic layers (e.g. o and t for CdI_2) and of some specific f-type layers occurring between the basic layers. In other words, polytypes are interpolytype structures (intermediate between $2H$ and $4H$ for CdI_2) with some interpolytype faults (phase boundaries) occurring in the polytype–polytype interface (basic polytypes are here represented by sequences of basic layers, e.g. o and t corresponding to $2H$ and $4H$). It should be noted that the lattices of $2H$ and $4H$ do not match each other completely: between the sequences $ooo\ldots$ ($2H$) and $ttt\ldots$ ($4H$) one or several molecular layers other than o and t have to occur (Pałosz, 1983c; Pałosz & Przedmojski, 1984).

To derive the geometrically possible and simultaneously the most probable structures for multilayer polytypes of SnS_2, we use here the multiphase model of polytype structure applied earlier to CdI_2 and PbI_2 (Pałosz, 1983c). In the case of SnS_2, having the three basic structures $2H$, $4H$ and $18R$, interpolytype two- and three-phase structures are possible: $2H$–$4H$, $2H$–$18R$, $4H$–$18R$ and $2H$–$4H$–$18R$. Interpolytype structures $2H$–$4H$ are common with CdI_2; the rules for constructing polytypes of this kind were discussed elsewhere and are not repeated here (Pałosz, 1982a, 1983c). General formulae of stacking sequences for other mixed structures predicted for SnS_2 are presented in the first column of Table 2. The stackings of layers in the polytype cells are also given. These theoretical sequences may be compared with the structural series of polytypes of CdI_2 by Pałosz (1982a, 1983c). In addition to the simple cell polytypes presented in Table 2 more complicated polytypes may occur in crystals, e.g. a hexagonal cell may be composed of several hexagonal or rhombohedral cells, a rhombohedral cell may consist of several hexagonal and/or rhombohedral

cells, *etc.* (Pałosz, 1982*a*). Earlier studies of already known polytypes of CdI_2, PbI_2 and $Ti_{1.2}S_2$ (Pałosz, 1983*c*) showed that most polytypes occurring in real crystals have a very simple composition. Because of this the presentation of polytype series in Table 2 is limited to the simplest polytype series predicted for SnS_2. The classification of polytype structures given in Table 2 formed the basis for the identification of 21 SnS_2 polytypes.

Structures of 21 polytypes of SnS_2

The intensities of 10.*l* and 1̄1.*l* reflexions measured on *a**-axis oscillation photographs, and normalized with the use of the absorption factor A^{-1}, for 21 multilayer

Table 2. *Series of polytypes of* SnS_2 *(intermediate structures 2H–4H–18R)*

Basic polytypes of SnS_2, 2*H*, 4*H* and 18*R*, are described in the *t–o–f* notation by the symbols *o*, *t* and *f*1*f*5*f*1, respectively. In a unit cell of 2*H* one *o* layer occurs, in a 4*H* cell two *t* layers occur, and a unit cell of 18*R* is composed of three *f*1*f*5*f*1 sequences occurring one after another.

Symbol of series	*t–o–f* sequence of a unit cell	Notes
	Polytypes 2*H*–18*R*	
	...*f*1*f*5*f*1(*o*)_*n*·*f*1*f*5*f*1(*o*)_*n*'·*f*1*f*5*f*1(*o*)_*n*·...	
Rhombohedral polytypes		
Sn*R*–1	(*f*1*f*5*f*1(*o*)_*n*)₃	*n* = 0, 1, 2,...
Sn*R*–2	(*f*1*f*5*f*1(*o*)_*n*·*f*1*f*5*f*1(*o*)_*n*')₃	*n* ≠ *n*'
Hexagonal polytypes		
		n = *n*' ≠ *n*''
Sn*H*–1	*f*1*f*5*f*1(*o*)_*n*·*f*1*f*5*f*1(*o*)_*n*'·*f*1*f*5*f*1(*o*)_*n*''	or
		n ≠ *n*' ≠ *n*''
	Polytypes 4*H*–18*R*	
	...(*t*)_*N*·*f*5(*t*)_*N*'·*f*1*f*1(*t*)_*N*'''·*f*5(*t*)_*N*''·*f*1*f*1(*t*)_*N*'''...	
Sn*R*–3	((*t*)_{2*N*}·*f*5(*t*)_{2*N*'}·*f*1*f*1)₃	*N*, *N*' = 0, 1, 2....
		N = *N*' ≠ *N*'' = *N*'''
Sn*R*–4	((*t*)_{2*N*}·*f*5(*t*)_{2*N*'}·*f*1*f*1(*t*)_{2*N*''}·*f*5(*t*)_{2*N*'''}·*f*1*f*1)₃	or
		N ≠ *N*' ≠ *N*'' = *N*''' *etc.*
Sn*H*–2	((*t*)_{2*N*+1}·*f*5(*t*)_{2*N*'+1}·*f*1*f*1	
Sn*H*–3	(*t*)_{2*N*}·*f*5(*t*)_{2*N*'}·*f*1*f*1(*t*)_{2*N*''}·*f*5(*t*)_{2*N*'''}·*f*1*f*1	
	Polytypes 2*H*–4*H*–18*R*	
	...(*t*)_*N*·*f*5(*t*)_*N*·*f*1(*o*)_*n*·*f*1(*t*)_*N*'·*f*5(*t*)_*N*'·*f*1(*o*)_*n*·*f*1...	
Sn*R*–5	((*t*)_{2*N*}·*f*5(*t*)_{2*N*'}·*f*1(*o*)_*n*·*f*1)₃	
Sn*H*–4	(*t*)_{2*N*+1}·*f*5(*t*)_{2*N*'+1}·*f*1(*o*)_*n*·*f*1 *etc.*	

polytypes of SnS_2 are plotted in Figs. 2(*a*)–2(*u*).* These figures compare the measured and calculated intensities for the polytypes under investigation. As seen in Fig. 2 the intensity diagrams have a very characteristic shape and identification of the polytypes appeared very simple. As is well known, polytypes containing large 'blocks' of a given simple structure (usually a basic polytype) give patterns in which the highest-intensity reflexions occur at the positions corresponding to the basic structure (or close to these positions). On this basis we have quickly indentified the polytypes presented in Figs. 2(*b*) to 2(*e*), 2(*g*), 2(*h*), 2(*j*), 2(*k*) and 2(*q*) as 2*H*-based structures and those presented in Figs. 2(*i*), 2(*l*), 2(*o*), 2(*r*) to 2(*u*) as 18*R*-based structures. (For comparison, in Fig. 1 intensity diagrams for the basic polytypes 2*H*, 4*H* and 18*R* are presented.) The rules for the construction of hexagonal and rhombohedral polytypes presented in Table 2 in the form of polytype cell formulae allowed us to identify these polytypes after calculations performed for only a few models. In particular, only one model was considered for the polytype 20*H* after identifying this polytype as an 18*R*-based structure (see series Sn*H*–1, Table 2). Similarly, just one model was considered for the identification of each of the layer stackings for the polytypes 10*H*₁, 38*H*₁, 56*H*₁, 74*H*₁, 24*R*₁ and 30*R*₁. For the rest of the polytypes, in no case were more than five models found necessary for the same purpose.

Discussion. Both the geometrical conditions of the construction of the crystal lattice and its stability decide the possible structure of a crystal. These two aspects are taken into account in the screw-dislocation theory of polytypism of Frank and in the theory of Jagodzinski, who suggested a layer-transposition mechanism for polytype formation (Verma & Krishna, 1966). As discussed many times in the literature (Trigunayat,
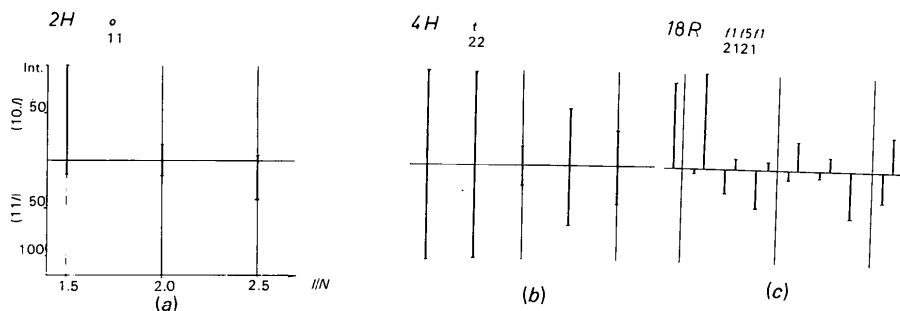
Fig. 1. Diagrams of intensities of reflexions 10.*l* and 1̄1.*l* calculated for basic polytypes of SnS_2: 2*H*, 4*H* and 18*R*.

1971; Pandey & Krishna, 1975; Prasad, 1976; Pałosz, 1983*b,c*), the screw-dislocation theory leads in some cases to an erroneous interpretation of the origin of polytypism. The theory of Jagodzinski is rather speculative and as such it cannot be the basis for a serious discussion of the reasons for polytypism.

Recently we discussed the structure of polytype crystals of MX_2 type without regard to the role the dislocations can play in the polytype formation (Pałosz, 1983*b,c*). The classifications of polytypes elaborated theoretically for multilayer polytypes as multiphase structures, for CdI_2 and PbI_2 (Pałosz, 1982*a*) and $Ti_{1.2}S_2$ (Pałosz, 1982*b*) and here for SnS_2, are fully confirmed experimentally. The multiphase character of polytypism is especially clearly seen for SnS_2 polytypes.

All known polytypes of SnS_2 (presented in this work) are constructed of layers o, t, $f1f5f1$ which correspond to the basic structures $2H$, $4H$ and $18R$, respectively. The stackings of layers corresponding to these basic structures are presented in Fig. 3. In Fig. 4 the construction of mixed sequences o–$f1f5f1$ and t–$f5f1f1$ occurring in polytype structures of SnS_2 is given. As seen in this figure the mixed sequences o–$f1f5f1$ and t–$f5f1f1$ occur without other sequences in the interface between the blocks of $2H$ and $18R$ and also between $4H$ and $18R$. This situation is quite different from that in CdI_2 or PbI_2 polytypes, where notations differing from that of the basic structures have to be used for describing the stacking of interfaces, *i.e.* $f1$, $f2$, $f5f1$ or $f4f2$ between $2H$ and $4H$ blocks in CdI_2 polytypes. It should be noted that in SnS_2 crystals the polytypes $2H$ and $4H$ occur simultaneously (in coalescence) similarly as in CdI_2 and PbI_2; however, here no multilayer polytypes having mixed structures $2H$–$4H$ (o–t) with interpolytype boundaries $f1$, $f2$, $f5f1$ or $f4f2$ were found. So, while in the case of CdI_2 and PbI_2 polytypism is closely connected with the creation of interpolytype $2H$–$4H$ boundaries (faults in the $2H$–$4H$ interface), in SnS_2 polytypes no stackings other than those corresponding to the basic structures occur.
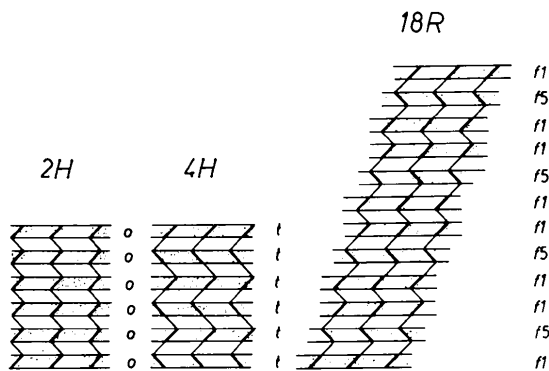

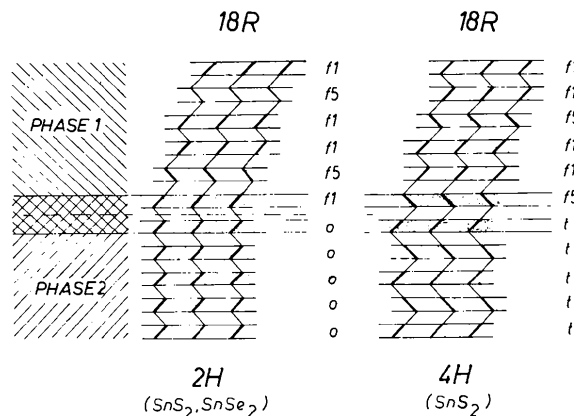Fig. 3. Structure of basic polytypes of SnS_2; stacking of X–M–X molecules in the (11.0) plane.

Fig. 4. Construction of interpolytype boundaries $2H$–$18R$ and $4H$–$18R$ occurring in polytype structures of SnS_2; stacking of X–M–X molecules in the (11.0) plane.

It is clear that differences between the polytypism of CdI_2, PbI_2, $Ti_{1.2}S_2$ and SnS_2 cannot be explained on the basis of the dislocation theory of polytypism. Growth of only some specific polytype structures, characteristic for a given material, suggests not only qualitative but also quantitative differences between structures occurring in one material and also between different compounds. It seems that the numerous theories of polytypism presented to date were not successful because of their mere qualitative character.

Final remarks

It might seem a little strange that polytypes occurring in SnS_2 have cells far larger than those typical for CdI_2 and PbI_2 polytypes (Pałosz, 1983*c*). Such a relation follows directly from the model of polytypism assuming that polytypes are interpolytype structures but not faulted basic polytypes. As shown, hexagonal polytypes of CdI_2 – intermediate $2H$–$4H$ structures – may have very small cells, *e.g.* $6H$: $tf1f2$, $8H$: $tf1of2$ (Pałosz, 1983*c*). The polytypes corresponding to them in SnS_2 – $2H$–$18R$ structures – are $20H$: $(f1f5f1)_3o$ and $38H$: $(f1f5f1)_6o$.

For CdI_2 and PbI_2 a correlation was found between the number of layers o and t occurring in complex polytype cells and the relative stabilities of the basic structures $2H$ and $4H$ (Pałosz, 1983*c*; Pałosz & Przedmojski, 1984). Similar correlations were found for SnS_2: polytypes corresponding to intermediate $2H$–$18R$ structures grow simultaneously with the pure polytypes $2H$ and $18R$; several polytypes of the type $2H$–$4H$–$18R$ found in SnS_2 occurred together with these three basic polytypes (Pałosz, Pałosz & Gierlotka, 1984). Determination of the effect of growth conditions on the stability of basic polytypes and on the construction of large-period polytypes requires the investigation of hundreds of crystals grown in different conditions. Such an investigation is now being undertaken and the results will be forthcoming.

References

FICHTNER, K. (1982). *Z. Kristallogr.* **159**, 311–313.
FICHTNER, K. (1983). *Cryst. Res. Technol.* **18**, 77–84.
GYANESHWAR, CHADHA, G. K. & TRIGUNAYAT, G. C. (1973). *Acta Cryst.* B**29**, 1791–1795.
LEE, J. D. & PAKES, H. W. (1969). *Acta Cryst.* A**25**, 712–713.
MINAGAWA, T. (1980). *J. Phys. Soc. Jpn*, **49**, 2317–2318.
MITCHELL, R. S., FUJIKI, Y. & ISHIZAWA, Y. (1974). *Nature (London)*, **247**, 537–538.
PAŁOSZ, B. (1980). *Z. Kristallogr.* **153**, 51–72.
PAŁOSZ, B. (1982a). *Acta Cryst.* B**38**, 3001–3009.
PAŁOSZ, B. (1982b). *Mater. Sci.* **8**, 29–41.
PAŁOSZ, B. (1983a). *Acta Cryst.* C**39**, 521–528, 1160–1163.
PAŁOSZ, B. (1983b). *Phys. Status Solidi A*, **77**, 11–34.

PAŁOSZ, B. (1983c). *Phys. Status Solidi A*, **80**, 11–41.
PAŁOSZ, B. & GIERLOTKA, S. (1984). *Z. Kristallogr.* **166**, 53–62.
PAŁOSZ, B. & PRZEDMOJSKI, J. (1980). *Z. Kristallogr.* **151**, 31–48.
PAŁOSZ, B. & PRZEDMOJSKI, J. (1984). *Cryst. Res. Technol.* **19**, 15–25.
PAŁOSZ, W., PAŁOSZ, B. & GIERLOTKA, S. (1984). International Conference on Crystal Growth and Characterization of Polytype Structures, Marseille.
PANDEY, D. & KRISHNA, P. (1975). *Philos. Mag.* 3̇**1**, 1113–1132.
PRASAD, B. (1976). *Phys. Status Solidi A*, **38**, 11–44.
TRIGUNAYAT, G. C. (1971). *Phys. Status Solidi A*, **4**, 281–299.
VERMA, A. R. & KRISHNA, P. (1966). *Polymorphism and Polytypism in Crystals.* New York: John Wiley.
WHITEHOUSE, C. R. & BALCHIN, A. A. (1979a). *J. Cryst. Growth*, **47**, 203–212.
WHITEHOUSE, C. R. & BALCHIN, A. A. (1979b). *Z. Kristallogr.* **149**, 241–247.
WIEDEMEIER, H. & CSILLAG, F. J. (1979). *J. Cryst. Growth*, **46**, 189–197.

Structure de l'Orthophosphate Acide de Thallium à Valence Mixte, $Tl_3\{Tl_{0,5}(H_3O)_{0,5}\}H_{14}(PO_4)_8.4H_2O$

PAR M. CHIADMI, J. VICAT, D. TRAN QUI ET A. BOUDJADA

Laboratoire de Cristallographie, CNRS, Laboratoire associé à l'USMG, 166 X, 38042 Grenoble CEDEX, France

Abstract. $M_r = 1570 \cdot 7$, triclinic, $P\bar{1}$, $a = 9 \cdot 820$ (8), $b = 9 \cdot 973$ (6), $c = 17 \cdot 87$ (1) Å, $\alpha = 90 \cdot 14$ (2), $\beta = 90 \cdot 01$ (1), $\gamma = 119 \cdot 46$ (4)°, $V = 1523$ (5) Å³, $Z = 2$, $D_x = 3 \cdot 42$ Mg m^{-3}, Ag $K\alpha$, $\lambda = 0 \cdot 5608$ Å, $\mu = 10 \cdot 65$ mm^{-1}, $F(000) = 1438$, room temperature, $R = 0 \cdot 07$, $wR = 0 \cdot 08$ for 3589 independent reflections and 433 variable parameters. Structure analysis has suggested a formula $Tl_3^{3+}\{Tl_{0.5}^+(H_3O^+)_{0.5}\}H_{14}(PO_4)_8.-4H_2O$, in which PO_4 planes perpendicular to the c axis alternate with the thallium and water planes. The three Tl^{3+} are octahedrally coordinated by oxygen atoms with Tl^{3+}—O distances varying from $2 \cdot 18$ (2) to $2 \cdot 25$ (2) Å while Tl^+ ions are surrounded by eight oxygen atoms with Tl^+—O distances in the range $2 \cdot 90$ (2) to $3 \cdot 12$ (2) Å.

Introduction. Les orthophosphates de thallium monovalent ont été l'objet de nombreuses études structurales (Oddon, 1979), par contre les études structurales de l'orthophosphate de thallium trivalent sont rares.

Récemment, l'étude du diagramme ternaire Tl_2O_3–P_2O_5–H_2O à 298 K (Khomutova, Fakeev & Zakharchenko, 1980) a permis de mettre en évidence cinq composés: $Tl_2O_3.P_2O_5.4H_2O$; $Tl_2O_3.2P_2O_5.9H_2O$; $Tl_2O_3.2P_2O_5.7H_2O$; $Tl_2O_3.2P_2O_5.5H_2O$; $Tl_2O_3.-3P_2O_5.6H_2O$.

La seule structure connue parmi ces composés est celle de $TlPO_4.2H_2O$ (Khomutova *et al.*, 1980). Dans notre laboratoire, lors des essais de synthèse d'orthophosphates acides dans le cadre de la recherche de nouveaux matériaux conducteurs protoniques, nous avons mis en évidence une nouvelle phase d'orthophosphate de thallium trivalent dont nous décrivons ici la structure cristalline.

Partie expérimentale. Synthèse des cristaux réalisée en laissant réagir l'oxyde de thallium, Tl_2O_3, avec une solution d'acide orthophosphorique H_3PO_4 à la température ambiante. Au bout de quatre à cinq semaines, on obtient des plaquettes hexagonales transparentes qui se clivent facilement en feuillets parallèles au plan (001). Cristaux sont hygroscopiques et instables en milieu ambiant. Etude cristallographique préliminaire sur chambre photographique de précession, groupe $P1$ ou $P\bar{1}$ avec une maille pseudo-hexagonale et une symétrie pseudo-monoclinique. Mesure des intensités sur cristal de forme hexagonale tronquée (Fig. 1) examiné au microscope polarisant pour vérifier l'absence de domaines dus à mâcle par pseudo-mériédrie, puis scellé dans tube capillaire. Paramètres de maille obtenus à partir des clichés de précession et de Weissenberg puis affinés par moindres carrés sur diffractomètre (24